Ultrafast band-gap oscillations in iron pyrite

Ultrafast band-gap oscillations in iron pyrite

Brian Kolb and Alexie M. Kolpak
Department of Mechanical Engineering, Massachusetts Institute of Technology, Cambridge, Massachusetts 02139, USA
(Received 7 August 2013; revised manuscript received 17 October 2013; published 20 December 2013)

With its combination of favorable band gap, high absorption coefficient, material abundance, and low cost, iron pyrite, FeS_2, has received a great deal of attention over the past decades as a promising material for photovoltaic applications such as solar cells and photoelectrochemical cells. Devices made from pyrite, however, exhibit open circuit voltages significantly lower than predicted, and despite a recent resurgence of interest in the material, there currently exists no widely accepted explanation for this disappointing behavior. In this paper, we show that phonons, which have been largely overlooked in previous efforts, may play a significant role. Using fully self-consistent GW calculations, we demonstrate that a phonon mode related to the oscillation of the sulfur-sulfur bond distance in the pyrite structure is strongly coupled to the energy of the conduction-band minimum, leading to an ultrafast ($\approx$100 fs) oscillation in the band gap. Depending on the coherency of the phonons, we predict that this effect can cause changes of up to $\pm$0.3 eV relative to the accepted FeS_2 band gap at room temperature. Harnessing this effect via temperature or irradiation with infrared light could open up numerous possibilities for novel devices such as ultrafast switches and adaptive solar absorbers.

DOI: 10.1103/PhysRevB.88.235208 PACS number(s): 71.15.Mb, 63.20.−e, 71.15.Pd, 71.20.Nr

I. INTRODUCTION

For over 30 years iron pyrite (fool's gold) has been investigated as a possible solar cell material. Interest in pyrite stems primarily from its favorable band gap[1] [0.95 eV (Ref. 3)], high absorption coefficient, relatively cheap and abundant elemental composition, and the environmentally benign nature of its components. The estimated price per watt of electricity generated from even a moderately efficient pyrite solar cell is tantalizing and has kept researchers looking into pyrite for decades. Despite its high promise, however, pyrite fails to perform in actual photoelectrochemical cells. Specifically, the best open circuit voltage yet obtained is around 200 meV,[4,5] much lower than expected for a material with a band gap of 0.95 eV, and not very conducive to a practical photovoltaic device.[6,7] Although this observation initially caused interest in pyrite to wane, there has been a resurgence in recent years as researchers try to explain the poor open circuit voltage with an aim toward engineering a solution. The literature is rich with possible explanations but to date no clear answer has been obtained, although bulk defects,[8–10] intrinsic surface states,[11–13] and the presence of competing phases,[11] most notably marcasite, have been largely ruled out as culprits. It is likely that surface defects play a significant role in the phenomenon.[10] Surface sulfur vacancies have been investigated in the past with relatively contradictory results,[10,12] but a recent study[14] lends credence to the assertion that they play a significant role in lowering the bulk band gap of pyrite.

Although much attention has been paid to the static properties of bulk pyrite, specifically its band gap and suitability as a photovoltaic material, relatively little attention has been directed toward its dynamic properties. It has been predicted that the positions of the atoms within the unit cell of pyrite, especially the sulfur-sulfur distance, have a large impact on its electronic structure.[15,16] It is not known, however, what form the position dependence of the band gap takes or what effect dynamic changes in these positions via phonons at finite temperature may have on the band gap of the material. In this work we seek to address these questions with a detailed analysis from first principles.

Herein we use fully self-consistent GW calculations coupled to density functional theory (DFT) to examine the effect of phonons on the band gap of pyrite. We find that the sulfur-sulfur distance plays a pivotal role in determining the band gap of the material and that phonons that change this distance create an oscillating band gap on an ultrafast timescale. The magnitude of the effect depends on temperature and other environmental conditions but it is predicted to create deviations of up to $\pm$0.27 eV from the average band gap at room temperature. We stress that this is an effect at a given temperature, distinct from the ubiquitous alteration of the band gap with changing temperature that is well known in semiconductor physics. The effect establishes a significant oscillation of the band gap at room temperature which persists, through zero point motion, even at 0 K. If this effect can be controlled, perhaps via input of infrared radiation to excite particular phonon modes, the material may be of use in applications such as ultrafast switching and adaptive solar absorbers. Conversely, suppression of these phonon modes by appropriate engineering may stabilize the band gap and lead to improved and more consistent device characteristics, although it remains to be seen whether band-gap oscillations on this time scale will in any way affect device performance.

II. METHODS

Density functional theory has been wildly successful at predicting a host of materials properties ever since its inception in the 1960s.[17,18] One major area in which it fails to perform, however, is in predicting semiconductor band gaps. Usage of the Kohn-Sham eigenvalues with most common functionals within DFT fails to produce band gaps close to experiment, usually underestimating them by a significant amount. More elaborate methods are generally required if one is to compute an accurate band gap from first principles.

Many attempts have been made to combat this shortcoming of DFT, including the GW approximation, many-body

perturbation theory, time-dependent density functional theory, hybrid functionals fit to reproduce band gaps, the modified Becke-Johnson potential,[19] the Δ-sol method,[20] the Hubbard-U correction, and others. Many of these approaches use empirically determined parameters fit to a particular data set and, as such, are not truly *ab initio*. The GW method is a quasiparticle Green's-function approach in which the electrons along with their surrounding polarization cloud are treated as weakly interacting particles. The method, which is fully *ab initio*, has been shown to reproduce band gaps with good accuracy in a host of semiconducting and insulating systems.[21,22] In the GW method, the self-energy is expanded to first order in the screened Coulomb interaction. Computing the screening requires knowledge of the electronic states in the material. Typically, DFT orbitals are used as a starting point for the calculation of the Green's function and the dynamical screening. This so-called G_0W_0 approach, however, suffers from a dependence on the functional used to generate the orbitals. This starting-point dependence can be removed by computing the screened Coulomb interaction and the interacting Green's function self-consistently. It is generally agreed that, when energies and orbitals are iterated to self-consistency within the GW, approach the result is a starting-point independent band gap that is among the best that current theory can provide.

In this work, fully self-consistent GW calculations were performed on iron pyrite using the Vienna Ab Initio Simulation Package (VASP).[23,24] An energy cutoff of 600 eV was used for the initial DFT runs along with an SCF convergence criterion of 1×10^{-8} eV and a Γ-centered $3 \times 3 \times 3k$-point mesh. This relatively coarse k-mesh, while not ideal, is necessary to make the expensive GW calculations tractable. Nevertheless, it is well sufficient to converge band gaps since the conduction-band minimum occurs at the Γ point, which is included in the mesh, and the valence band is relatively flat throughout the Brillouin zone. Projector augmented wave potentials were used as supplied with VASP.[25,26] Iron pseudopotentials included $3s$ and $3p$ semicore states. DFT runs utilized generalized gradient approximation (GGA) exchange correlation as laid out by Perdew, Burke, and Ernzerhof (PBE).[27] Relaxations were carried out until all forces were less than 1 meV/Å. For the GW calculations, an energy cutoff of 200 eV was used. To properly account for screening, one must calculate a significant number of unoccupied bands. In this work, 520 unoccupied bands were used for the screening calculations. The GW energies and orbitals were iterated until each eigenvalue changed by less than 0.01 eV.

For all systems other than iron pyrite itself (FeS_2) band gaps were calculated using one-shot G_0W_0 starting from well-converged PBE0 hybrid orbitals and energies. In several cases, fully self-consistent calculations were carried out and, in most cases, the results did not differ appreciably from the G_0W_0 results presented here. Other than the use of PBE0 to G_0W_0, the computational parameters for these systems were identical to those described above for pyrite.

III. RESULTS AND DISCUSSION

After much debate in the literature, it is now widely accepted that pyrite exhibits an indirect band gap of 0.95 eV,

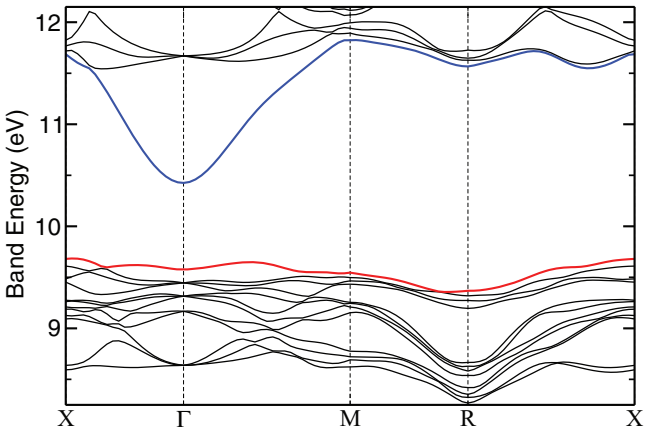

FIG. 1. (Color online) The GW-calculated band structure of iron pyrite at the PBE-relaxed geometry. The valence band is shown in red and the conduction band is shown in blue.

with the conduction-band minimum occurring at the Γ point. Figure 1 shows the GW-calculated band structure of pyrite (interpolated using Wannier90) at the PBE-relaxed geometry. At this geometry ($a = 5.40$ Å, $u = 0.382$) the predicted band gap is 0.83 eV, in agreement with previous GW calculations of pyrite. However, when the experimental geometry is used ($a = 5.42$ Å, $u = 0.384$) the GW-computed band gap rises to 1.01 eV, in good agreement with the accepted value. The difference in band gap between the two structures is rooted in the unique configuration of the pyrite structure. The structure contains iron atoms on an fcc lattice with interstitial sulfur-sulfur covalent dimers. These sulfur-sulfur covalent bonds are oriented along the ⟨111⟩ directions of the crystal with the center of mass of the dimers forming an fcc lattice that interpenetrates the iron fcc lattice. Thus, the pyrite structure consists of an unusual mixture of both metal-chalcogenide bonds and short chalcogen-chalcogen covalent bonds. The covalent bonds are key to the dynamical properties of the pyrite band gap.

A close look at the conduction-band minimum shows the origin of the geometrical dependence of the band gap. The conduction-band minimum is comprised of sulfur p σ^* antibonding states, as evidenced in Fig. 2. Bringing the covalently bound sulfur atoms closer together thus raises the energy of the conduction-band minimum. Conversely, increasing the separation between covalently bound sulfur atoms lowers the energy of the conduction-band minimum. The energies of the conduction-band minimum (CBM) and valence-band maximum (VBM) as a function of the sulfur-sulfur distance are shown in the top panel of Fig. 3. The band structures associated with a decreased and increased sulfur-sulfur distance are shown in the bottom-left and -right panels, respectively. Note that the energy of the valence-band maximum, being comprised mainly of iron d orbitals, is relatively insensitive to the positions of the sulfur atoms while the conduction-band minimum moves up and down significantly as the sulfur-sulfur distance changes.

The strong sulfur-sulfur distance dependence of the band gap shown in Fig. 3 suggests that phonons affecting this distance might lead to a dynamically varying band gap with significant deviations from the static, equilibrium value. To test

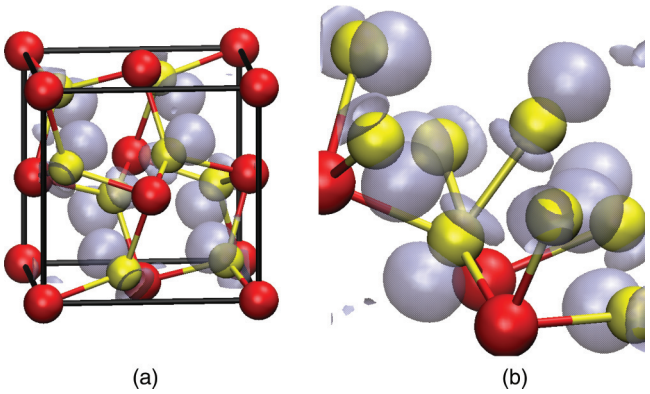

FIG. 2. (Color online) (a) The charge density arising from the state at the conduction-band minimum in pyrite. Red atoms are iron, yellow are sulfur, and the transparent blue is the charge density arising from the state. (b) The same as in (a) but zoomed in on a sulfur-sulfur covalent bond.

this assertion the Γ-centered phonons of pyrite were calculated with the PBE functional. There are a number of phonons that change the sulfur-sulfur distance, but most important is a mode at 347 cm^{-1} that simply corresponds to the oscillation of the covalently bound sulfur atoms with respect to each other. We predict that this phonon causes an oscillation of the pyrite band gap with a period of about 100 fs. The amplitude of this

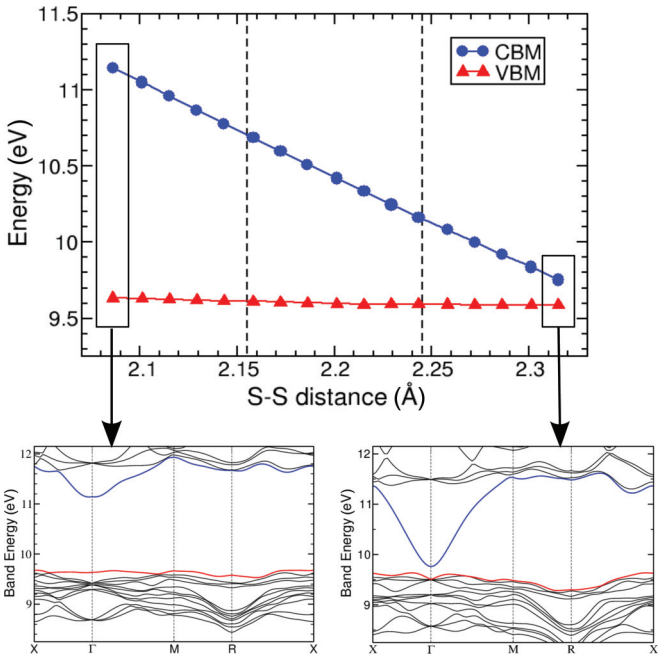

FIG. 3. (Color online) (top) *GW*-computed energies of the conduction-band minimum (CBM) and valence-band maximum (VBM) as a function of sulfur-sulfur distance. For this plot, all sulfur-sulfur distances in the unit cell were set to the indicated value. The vertical dashed lines demarcate the expected range of sulfur-sulfur distance at room temperature. Bottom left: Band structure of pyrite when the sulfur-sulfur distance is decreased by 5% from its PBE equilibrium value. Bottom right: Band structure of pyrite when the sulfur-sulfur distance is increased by 5% over its PBE equilibrium value.

oscillation will be temperature dependent, but its average value and frequency are not.

The amplitude of the band-gap oscillation at room temperature can be ascertained as follows. The population of a phonon of frequency ω at some temperature T is given by the Bose-Einstein relation

$$N_\omega = \frac{1}{e^{\hbar\omega/k_B T} - 1}. \quad (1)$$

This can be used to compute the energy in the mode via the familiar relation

$$E_\omega = \hbar\omega \left[N_\omega + \frac{1}{2} \right]. \quad (2)$$

Using Eqs. (1) and (2), the excitation energy of a particular phonon mode can be calculated at any given temperature. The range of band gaps associated with a coherent phonon of this mode can then be determined by displacing the system along the mode in each direction enough to raise its energy by the prescribed amount, followed by a *GW* computation of the band gap at the resulting geometry.

For the mode at 347 cm^{-1} such an analysis yields a change in the sulfur-sulfur distance of about ±0.045 Å at 300 K. The upper and lower bounds of the band gap during such an oscillation are 1.10 and 0.56 eV, respectively, relative to the 0.83-eV PBE equilibrium value. In other words, at room temperature, the band gap deviates by about ±0.27 eV from its average value over the course of one oscillation. These values are likely an upper bound on the room-temperature thermal oscillations, since in any real pyrite sample, different covalently bound sulfur atoms will be oscillating out of phase, i.e., the phonon mode will coexist with a concurrent population of other phonon modes, changing the sulfur-sulfur distances in complicated ways. Nevertheless, this upper bound, a total change in the band gap of over 0.5 eV, represents a staggering dependence of the band gap on thermal oscillations, even at room temperature.

To assess the bounds of the room-temperature thermal oscillation of the band gap in a more realistic sample of pyrite, a 10-ps *ab initio* molecular dynamics run was carried out on a 2 × 2 × 2 supercell (96 atoms) and the DFT band gaps were calculated for each configuration. The results of this analysis are presented in Fig. 4, which shows deviations from the average band gap of ±0.1 to ±0.15 eV. Unfortunately, the cost of *GW* calculations makes computation of the *GW* band gaps on such a supercell impractical. Nevertheless, although DFT consistently underestimates the value of the band gap, it exhibits the same trend of band gap with changing sulfur-sulfur distance as careful *GW* calculations, as verified by Fig. 5, which shows the GW and DFT band gaps of pyrite as a function of the sulfur-sulfur distance. Thus, the DFT band gaps in Fig. 4 are not meant to represent the true band gaps but are given as an indication of the magnitude of oscillations at 300 K. These oscillations could be made more extreme either by exciting the 347-cm^{-1} mode with infrared light to obtain coherent phonons or by raising the temperature of the pyrite sample. Since the role of a solar cell is to absorb radiation, it is likely that both of these effects will be present in real solar cells made from pyrite.

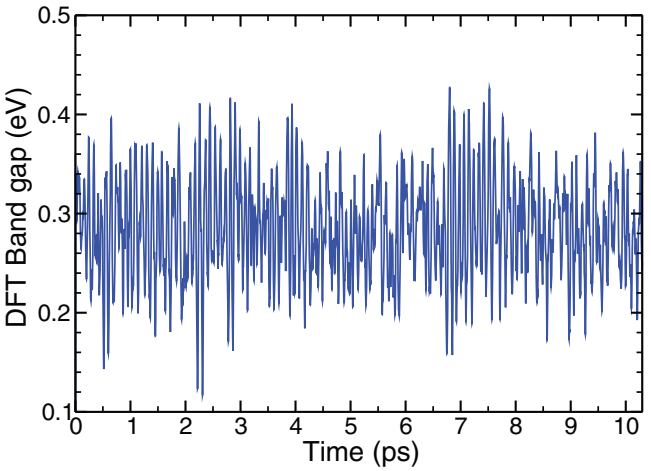

FIG. 4. (Color online) DFT-computed band gaps during an *ab initio* molecular dynamics run of a $2 \times 2 \times 2$ supercell of pyrite utilizing the PBE functional. Absolute values of the band gap are, of course, underestimated but changes in band gap are predicted correctly.

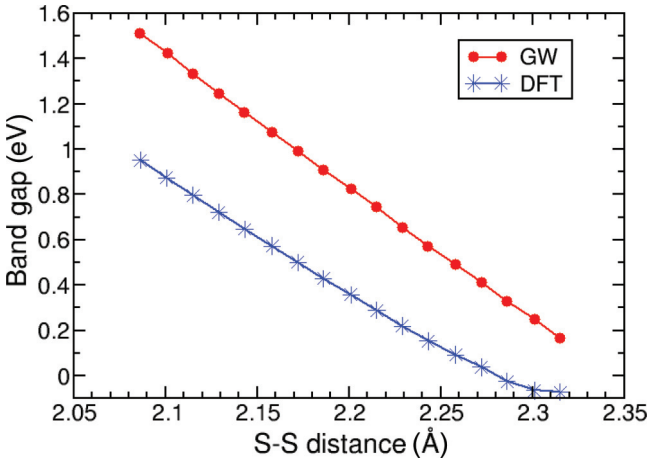

FIG. 5. (Color online) Band gap of pyrite as a function of sulfur-sulfur distance as calculated by both GW (red circles) and DFT (blue stars). The PBE-calculated equilibrium distance is 2.2 Å. Note that, although DFT predicts band gaps significantly lower than their GW counterparts, the changes in band gap with respect to sulfur-sulfur distance are predicted correctly, as long as DFT predicts a semiconducting state. This justifies our use of DFT band gaps to discuss the change in band gap at 300 K in Fig. 4 of the paper.

It is interesting to ask whether other inorganic materials with strong covalent bonds may also exhibit this effect. For example, there are dozens of materials that form in the pyrite structure; most of these are metallic but there are a number that are semiconducting. From an investigation of the band structures of these materials we predict that similar band-gap oscillations will exist in 13 other experimentally realizable compounds of iron, ruthenium, osmium, zinc, cadmium, and magnesium with the chalcogenides (S, Se, and Te), all of which have the pyrite structure. Table I gives the GW band gaps at both the experimental and PBE-relaxed geometries and the period of the main phonon responsible for changes in the chalcogen-chalcogen distance for each of these systems. All of the tabulated systems exhibit the same parabolic conduction band with a conduction-band minimum at Γ, comprised of chalcogen p antibonding orbitals.

Note that the relaxed band gaps are, in all cases, different from their experimental-geometry counterparts. This is because the PBE functional (and, in fact, almost a dozen other functionals tried) tends to get the chalcogen-chalcogen distance wrong by at least a few percent as compared to experimental geometries. Even this relatively small error can have significant consequences for the band gaps in these systems in which the energy of the conduction-band minimum is so sensitive to atomic positions. The unfortunate side effect

TABLE I. Semiconducting systems which form in the pyrite structure and are predicted to exhibit an oscillating band gap. Given in the table are the GW-computed band gap at the experimental geometry (E_g^{expt}) (experimental values given in parentheses), the period of the phonon mode that directly changes the chalcogen-chalcogen distance, the GW-computed value of the band gap at the PBE-relaxed geometry (E_g^{relax}), and the predicted minimum ($\Delta E_g{}^-$) and maximum ($\Delta E_g{}^+$) excursions of the band gap at room temperature.

Compound	E_g^{expt} (eV)	Period of phonon (fs)	E_g^{relax} (eV)	$\Delta E_g{}^-$	$\Delta E_g{}^+$ (eV)
FeS_2	1.01 [0.95 (Ref. 3)]	96	0.83	−0.27	0.27
$FeSe_2$	0.76	160	0.05	metallic	0.31
$FeTe_2$	0.11	209	metallic	metallic	metallic
RuS_2	1.38 [1.33 (Ref. 28)]	95	1.21	−0.31	0.31
$RuSe_2$	0.83 [0.76 (Ref. 29)]	155	0.65	−0.25	0.25
$RuTe_2$	0.36 [0.37 (Ref. 30)]	230	0.3	−0.24	0.23
OsS_2	0.75 [2.0[a] (Ref. 31)]	104	0.39	−0.33	0.38
$OsSe_2$	0.67	162	0.11	metallic	0.26
$OsTe_2$	0.15	201	0.08	metallic	0.21
ZnS_2	3.09	69	3.59	−0.19	0.05
$ZnSe_2$	2.25	129	2.5	−0.16	0.06
CdS_2	2.41	66	3.25	−0.05	0.03
$MgSe_2$	3.62	128	3.76	−0.18	0.1
$MgTe_2$	2.50	191	2.46	−0.16	0.15

[a]This measurement, reported in 1963, is labeled in the original article as approximate and preliminary. No further experimental measurements could be found and this number is commonly cited.

of this error is that, in some systems, the relaxed structure (which is required to compute the phonons) or the structure perturbed along a phonon mode turns out to be incorrectly metallic. In these cases the range of band-gap oscillations cannot be fully predicted. For the remaining systems, Table I gives the predicted upper ($\Delta E_g{}^+$) and lower ($\Delta E_g{}^-$) deviations in band gap corresponding to coherent phonons at room temperature.

IV. CONCLUSION

GW calculations were performed on iron pyrite, FeS_2, to examine the nature of the band structure and determine its dynamic behavior. The presence of covalently bound sulfur dimers in the pyrite structure gives rise to a parabolic conduction band with a minimum comprised of the sulfur-sulfur antibonding *p* orbital. This results in a strong dependence of the energy of the conduction-band minimum on the sulfur-sulfur distance, which changes dynamically on a femtosecond time scale as a result of phonons within the material. Since the valence band, comprised mainly of iron *d* orbitals, is relatively unaffected by the changing sulfur-sulfur distance, this leads to band-gap oscillations on the order of tenths of electron volts over a period of ≈100 fs. The ultrafast period of these oscillations makes it unlikely that they will be observed with standard band-gap measurement techniques. More work is needed, however, to determine whether this phenomenon will have any detrimental effect on the performance of semiconducting devices made from pyrite. It is possible that novel devices could be devised that make use of this effect, especially given the wide range of materials that are predicted to exhibit it. We hope that the computational demonstration of this phenomenon will spur efforts to both experimentally measure the effect and to determine its impact on the performance of pyrite-based devices.

ACKNOWLEDGMENTS

The authors acknowledge computational support from the Extreme Science and Engineering Discovery Environment (XSEDE), which is supported by National Science Foundation Grant No. OCI-1053575, and financial support from the Advanced Research Projects Agency-Energy (ARPA-E), US Department of Energy, under Award No. DE-AR0000180.

[1]The band gap of pyrite was a source of considerable debate in the literature for over a decade, with experimental values ranging from 0.7 eV to greater than 2 eV (see Ref. 2 for an overview of this). Early work was done on natural samples and it is widely believed that the discrepancies originated from differences in composition between samples. The value of 0.95 eV quoted here is now widely accepted as the band gap of pure pyrite.

[2]I. J. Ferrer, N. D. M., C. de las Heras, and C. Sanchez, Solid State Commun. **74**, 913 (1990).
[3]A. Ennaoui, S. Flechter, H. Goslowsky, and H. Tributsch, J. Electrochem. Soc. **132**, 1579 (1985).
[4]A. Ennaoui and H. Tributsch, Sol. Cells **13**, 197 (1984).
[5]A. Ennaoui, S. Fiechter, W. Jaegermann, and H. Tributsch, J. Electrochem. Soc. **133**, 97 (1986).
[6]A. Ennaoui, S. Fiechter, C. Pettenkofer, N. Alonso-Vante, K. Büker, M. Bronold, C. Höpfner, and H. Tributsch, Sol. Energy Mater. Sol. Cells **29**, 289 (1993).
[7]K. Büker, N. Alonso-Vante, and H. Tributsch, J. Appl. Phys. **72**, 5721 (1992).
[8]J. Hu, Y. Zhang, M. Law, and R. Wu, Phys. Rev. B **85**, 085203 (2012).
[9]R. Sun, M. K. Y. Chan, S. Y. Kang, and G. Ceder, Phys. Rev. B **84**, 035212 (2011).
[10]L. Yu, S. Lany, R. Kykyneshi, V. Jieratum, R. Ravichandran, B. Pelatt, E. Altschul, H. A. S. Platt, J. F. Wager, D. A. Keszler, and A. Zunger, Adv. Energy Mater. **1**, 748 (2011).
[11]R. Sun, M. K. Y. Chan, and G. Ceder, Phys. Rev. B **83**, 235311 (2011).
[12]Y. N. Zhang, J. Hu, M. Law, and R. Q. Wu, Phys. Rev. B **85**, 085314 (2012).
[13]J. Cai and M. R. Philpott, Comput. Mater. Sci. **30**, 358 (2004).
[14]F. W. Herbert, A. Krishnamoorthy, K. J. V. Vliet, and B. Yildiz, Surf. Sci. **618**, 53 (2013).
[15]V. Eyert, K.-H. Höck, S. Fiechter, and H. Tributsch, Phys. Rev. B **57**, 6350 (1998).
[16]I. Opahle, K. Koepernik, and H. Eschrig, Phys. Rev. B **60**, 14035 (1999).
[17]P. Hohenberg and W. Kohn, Phys. Rev. **136**, B864 (1964).
[18]W. Kohn and L. J. Sham, Phys. Rev. **140**, A1133 (1965).
[19]A. D. Becke and E. R. Johnson, J. Chem. Phys. **124**, 221101 (2006).
[20]M. K. Y. Chan and G. Ceder, Phys. Rev. Lett. **105**, 196403 (2010).
[21]M. van Schilfgaarde, T. Kotani, and S. Faleev, Phys. Rev. Lett. **96**, 226402 (2006).
[22]M. Shishkin and G. Kresse, Phys. Rev. B **75**, 235102 (2007).
[23]G. Kresse and J. Furthmüller, Comput. Mater. Sci. **6**, 15 (1996).
[24]G. Kresse and J. Furthmüller, Phys. Rev. B **54**, 11169 (1996).
[25]P. E. Blochl, Phys. Rev. B **50**, 17953 (1994).
[26]G. Kresse and D. Joubert, Phys. Rev. B **59**, 1758 (1999).
[27]J. P. Perdew, K. Burke, and M. Ernzerhof, Phys. Rev. Lett. **77**, 3865 (1996).
[28]J. K. Huang, Y. S. Huang, and T. R. Yang, J. Phys.: Condens. Matter **7**, 4175 (1995).
[29]H. P. Vaterlaus, R. Bichsel, F. Lévy, and H. Berger, J. Phys. C: Solid State Phys. **18**, 6063 (1985).
[30]P. C. Liao, J. K. Huang, Y. S. Huang, and T. R. Yang, Solid State Commun. **98**, 279 (1996).
[31]F. Hulliger, Nature (London) **200**, 1064 (1963).